Characterization and photophysical properties of sulfur-oxidized diarylethenes

ARTICLE *in* TETRAHEDRON · MARCH 2007

Impact Factor: 2.64 · DOI: 10.1016/j.tet.2007.02.007

Available online at www.sciencedirect.com
ScienceDirect
Tetrahedron
Tetrahedron 63 (2007) 3173–3182

Characterization and photophysical properties of sulfur-oxidized diarylethenes

Yong-Chul Jeong,[a] Jun Pil Han,[a] Yongho Kim,[a] Eunkyoung Kim,[b,*] Sung Ik Yang[a,*] and Kwang-Hyun Ahn[a,*]

[a]*College of Environment and Applied Chemistry, and MRCID, Kyung Hee University, Yongin 449-701, Republic of Korea*
[b]*Department of Chemical Engineering, Yonsei University, 134 Shinchon-dong, Seodaemun-gu, Seoul 120-749, Republic of Korea*

Received 4 January 2007; revised 31 January 2007; accepted 2 February 2007
Available online 7 February 2007

Abstract—Controlled oxidation of sulfur atoms in benzothiophene rings of a photochromic diarylethene, 1,2-bis(2-methyl-1-benzothiophene-3-yl)perfluorocyclopentene (BTF6) by 3-chloroperbenzoic acid afforded various oxidation products such as BTFO1, BTFO2, and BTFO4. Upon irradiation with UV light, colorless o-BTFO1 and o-BTFO2 turned to red color, whereas colorless o-BTFO4 turned to yellow color. Theoretical calculation was performed to understand the absorption spectra of closed-ring isomers. All of those compounds returned back to their open-ring isomers upon irradiation with visible light. The cyclization conversions of BTFO*n* (*n*=1, 2, and 4) at the photostationary state are higher than that of BTF6. Interestingly, in the case of BTFO1, because of the unsymmetrical environment around the sulfoxide subunit in the molecule, the diastereoselective photocyclization was observed in 25% de. In addition, c-BTFO2 and c-BTFO4 also exhibited a marked fatigue resistance and strong fluorescence, respectively. Oxidation state of sulfur atom in a diarylethene can play an important role in determining its photophysical and photochromic properties.

1. Introduction

Photochromic materials have received a great attention because of their potentials in various applications including optoelectronics such as optical memory, switching, and display devices.[1] Diarylethene is one of the most well-known and extensively investigated classes of photochromic molecules because of its excellent thermally stable and fatigue resistant properties required for optoelectronic applications.[2] The photochromic reaction of diarylethenes is based on the reversible ring-closing and ring-opening reactions as shown in Scheme 1.[3] Upon irradiation with UV light, the open-ring isomer is converted into the closed-ring isomer, which has a new absorption band in the visible wavelength region. The closed-ring isomer reverts to the open-ring isomer upon irradiation with visible light. During the photochromic reactions, various physical properties such as refractive index,[4] optical rotation,[5] magnetic interaction,[6] IR peak intensity,[7] redox potential,[8] and fluorescence[9] as well as the absorption spectrum are changed. From the viewpoint of the optical memory and switching applications, the change in the physical properties can be utilized to achieve a non-destructive readout.[2a] Especially, the fluorescence change is an attractive method because of its high sensitivity.[9b,c] To optimize those physical properties for the purpose of a practical device application, various types of diarylethenes based on benzothiophene and thiophene have been synthesized and characterized. Recently, we reported that monosulfone (BTFO2) and disulfone (BTFO4) forms of a diarylethene obtained from an oxidation reaction of BTF6 by *m*CPBA showed interesting fatigue and fluorescence properties.[10] These results suggest that various properties represented by a diarylethene are strongly related with the oxidation state of sulfur atoms in the diarylethene. Thus, we tried to synthesize other oxidized forms of BTF6 and succeeded in isolating the monosulfoxo (BTFO1) form of BTF6 in a partial oxidation of BTF6 by *m*CPBA. Here, we would like to report the characterization of BTFO1 and its diastereoselective cyclization under light. Further, we want to describe the detailed photophysical properties of BTFO*n* (*n*=1, 2, and 4) that show an interesting tendency dependent upon the oxidation state of those diarylethenes.

2. Results and discussion

2.1. Synthesis and characterization of BTFO1

BTF6 [1,2-bis(2-methyl-1-benzothiophene-3-yl)perfluorocyclopentene] was prepared according to the procedure

Keywords: Photochromism; Diarylethene; Diastereoselective photocyclization; Fatigue property; Fluorescence readout; Sulfoxide.
* Corresponding authors. Tel.: +82 31 201 2447; fax: +82 31 202 7337; e-mail: khahn@khu.ac.kr

0040–4020/$ - see front matter © 2007 Elsevier Ltd. All rights reserved.
doi:10.1016/j.tet.2007.02.007

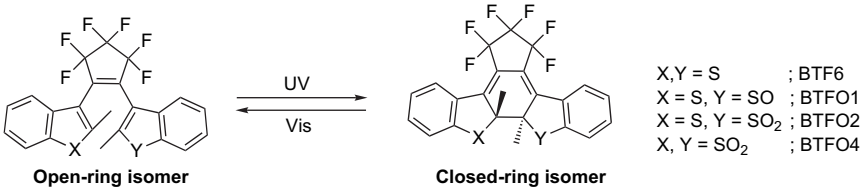

Scheme 1. Photochromic reaction of diarylethenes.

described in the literature.[4a,11] In the oxidation process of BTF6 to 1,2-bis(2-methyl-1-benzothiophene-1,1-dioxide-3-yl)perfluorocyclopentene (BTFO4)[10a] by 3-chloroperbenzoic acid (*m*CPBA), four different intermediates are expected as shown in Scheme 2. Among those four intermediates, 1-(2-methyl-1-benzothiophene-1,1-dioxide-3-yl)-2-(2-methyl-1-benzothiophene-3-yl)perfluorocyclopentene (BTFO2)[10b] had been isolated and characterized previously. In a continuing effort to obtain other intermediates, we were able to isolate the monosulfoxo-form of BTF6, 1-(2-methyl-1-benzothiophene-1-oxide-3-yl)-2-(2-methyl-1-benzothiophene-3-yl)-perfluorocyclopentene (BTFO1) from a reaction between BTF6 and 3-chloroperbenzoic acid (*m*CPBA) in relatively small yield, dependent upon the amount of oxidant used (Fig. 1). The structure of BTFO1 was confirmed with ^{1}H NMR and HRMS spectrometry. Especially, the crystal of BTFO1 in its open form state (o-BTFO1) was obtained from the hexane/ethyl acetate solution. Figure 2 shows the ORTEP drawing of the molecular structure of o-BTFO1. The ORTEP drawing indicates that the crystal of o-BTFO1 was unfortunately packed in the parallel (p) conformation that could not lead to the closed form upon UV irradiation.[12] The relative ratio of BTFO1, BTFO2, and BTFO4 that can be isolated in the oxidation of BTF6 is varied dependent upon the amount of *m*CPBA used as shown in Figure 1. Interestingly, in the oxidation reaction of BTF6 with 1 equiv of *m*CPBA, BTFO2 was obtained as a major product, indicating the nucleophilic character of *m*CPBA.[13] The oxidation rate of sulfoxide (BTFO1) to sulfone (BTFO2) by *m*CPBA must be faster than the oxidation rate of sulfide (BTF6) to sulfoxide (BTFO1).

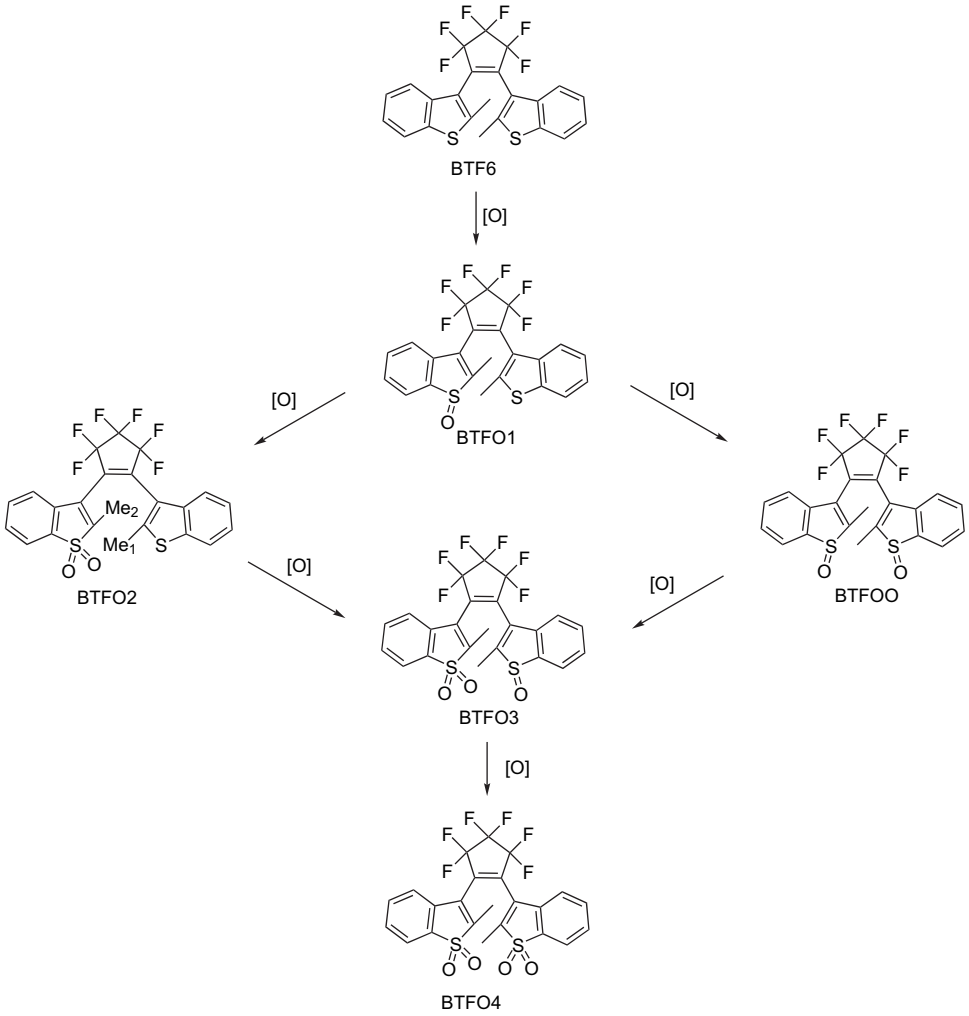

Scheme 2. Oxidation of BTF6.

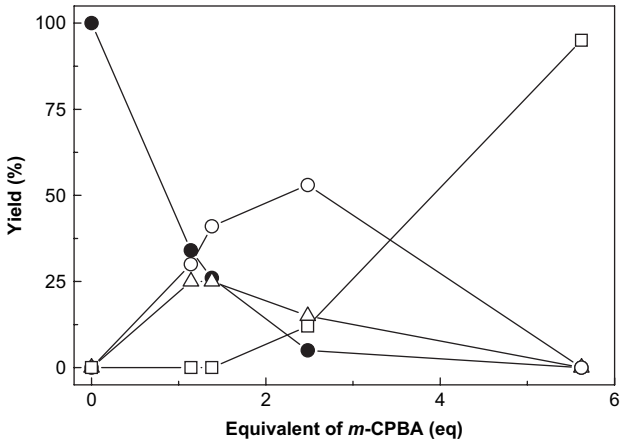

Figure 1. Distribution of BTFO*n* in an oxidation reaction of BTF6 by various amount of *m*CPBA (BTF6, closed circle; BTFO1, open triangle; BTFO2, open circle; BTFO4, open square).

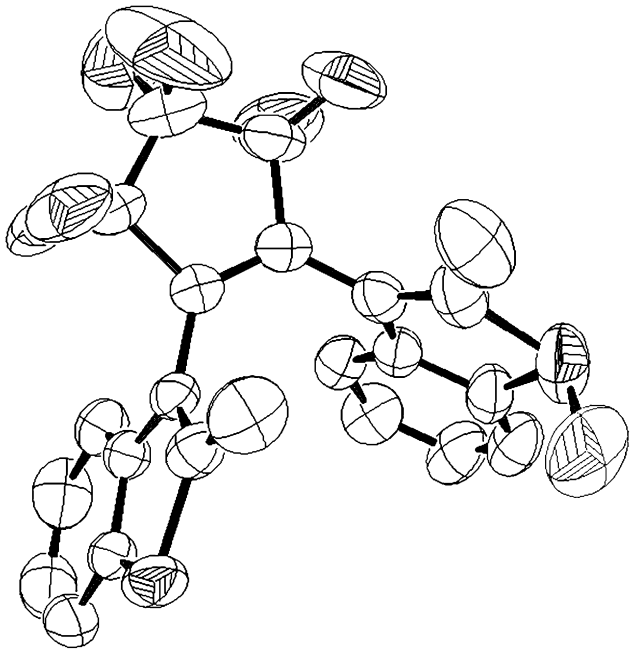

Figure 2. ORTEP drawing of o-BTFO1 with 50% probability ellipsoids. Hydrogen atoms are omitted for clarity.

2.2. ^{1}H NMR characterization of BTF6 and BTFO*n*

In the ^{1}H NMR of the open-ring isomer of BTF6 (o-BTF6), two methyl signals of p- and ap-conformation were observed at 2.49 and 2.21 ppm, respectively,[14] and their relative intensity, which is related to the relative population between p- and ap-conformer is 35:65. The ^{1}H NMR of the open-ring isomer of BTFO4 (o-BTFO4) also showed two methyl signals of p- and ap-conformer at 2.20 and 2.06 ppm, respectively, and their relative population was 50:50. Upon irradiation at 312 nm light, a new singlet peak corresponding to the ring-closed isomer of BTFO4 (c-BTFO4) was appeared at 1.85 ppm. In the ^{1}H NMR of o-BTFO2, four methyl signals with similar intensities were observed at 2.43, 2.30, 2.26, and 1.92 ppm. To characterize the methyl signals, HSQC experiment of the o-BTFO2 was performed. From the correlation obtained from the HSQC experiment of o-BTFO2, two peaks at 2.43 and 2.30 ppm correspond to Me_1 of p- and ap-conformation, and two peaks at 2.26 and 1.92 ppm correspond to Me_2 of p- and ap-conformation, respectively (Scheme 2). The intensities of those peaks were decreased upon irradiation with 312 nm light along with the appearance of new peaks of closed-ring isomer, c-BTFO2 at 1.90 and 1.61 ppm.

Since the open-ring form of BTFO1 (o-BTFO1) has a chiral center at its sulfoxide subunit, it is a mixture of four different rotational isomers and their enantiomers as shown in Scheme 3. Thus, it is expected to observe eight methyl groups in ^{1}H NMR of o-BTFO1.[5c] However, ^{1}H NMR of o-BTFO1 shows only six methyl signals at 2.53, 2.45, 2.31, 2.29, 2.11, and 2.09 ppm as shown in Figure 3A. The peaks can be assigned from the HSQC experiment as Me_1 of p-conformers **A** and **B** (2.53 and 2.45 ppm), Me_1 of *anti*-parallel (ap)-conformers **C** and **D** (2.31 and 2.29 ppm), Me_2 of p-conformer (2.45 and 2.31), and Me_2 of ap-conformer (2.11 and 2.09 ppm). From the NMR analysis, the relative population between the p- and ap-conformer was found to be 43:57. In order to have an idea about the major rotational isomer of o-BTFO1, the heat of formations of conformers **A**, **B**, **C**, and **D** were calculated using an AM1 program of MOPAC Ver. 7.0 (parentheses in Scheme 3). From these calculations, p-conformer **A** is favored over another p-conformer **B**, and ap-conformer **C** is more stable than another ap-conformer **D** of o-BTFO1. Based on the result, methyl signals of each isomers in the ^{1}H NMR could be assigned and the relative populations were determined to be 24, 19, 34, and 23 for **A**, **B**, **C**, and **D**, respectively. Upon illumination with 312 nm light to the o-BTFO1 in ethyl acetate, four new peaks appeared at 2.00, 1.80, 1.49, and 1.40 ppm (Fig. 3B), that may be related with the photocyclization of o-BTFO1 by the light. Since the closed-ring isomer of BTFO1 (c-BTFO1) is a mixture of two diastereomers such as *syn*-c-BTFO1 [(*R*,*S*,*S*)- and (*S*,*R*,*R*)-c-BTFO1] and *anti*-c-BTFO1 [(*S*,*S*,*S*)- and (*R*,*R*,*R*)-c-BTFO1] as shown in Scheme 3 and each diastereomer may show two methyl peaks in ^{1}H NMR, four singlet peaks in ^{1}H NMR must be the resonances of four methyl protons of those two diastereomers. From the peak intensity difference, it is expected that the diastereomer with methyl resonances at 1.80 and 1.49 ppm may be more stable than the isomer with those at 2.00 and 1.40 ppm. Based on the calculation of heat of formation, *syn*-c-BTFO1 is expected to be the major closed-ring diastereomer of c-BTFO1. Thus, the photocyclization of o-BTFO1 with 312 nm light resulted in the diastereoselective formation of *syn*-c-BTFO1 with 25% de calculated from the intensities of the ^{1}H NMR. Since the diastereoselective electrocyclization of polyene system containing a chiral sulfoxide has not been well studied, more studies are needed to improve the selectivity.

2.3. Photochromism of BTFO*n*

The absorption spectra of BTFO1, BTFO2, and BTFO4 in ethyl acetate (1.0×10^{-5} M) at room temperature are shown in Figure 4. For comparison, absorption spectrum of BTF6 reported previously is also included in Figure 4.[6c] Upon irradiation with 312 nm light, the colorless solutions of o-BTF6,

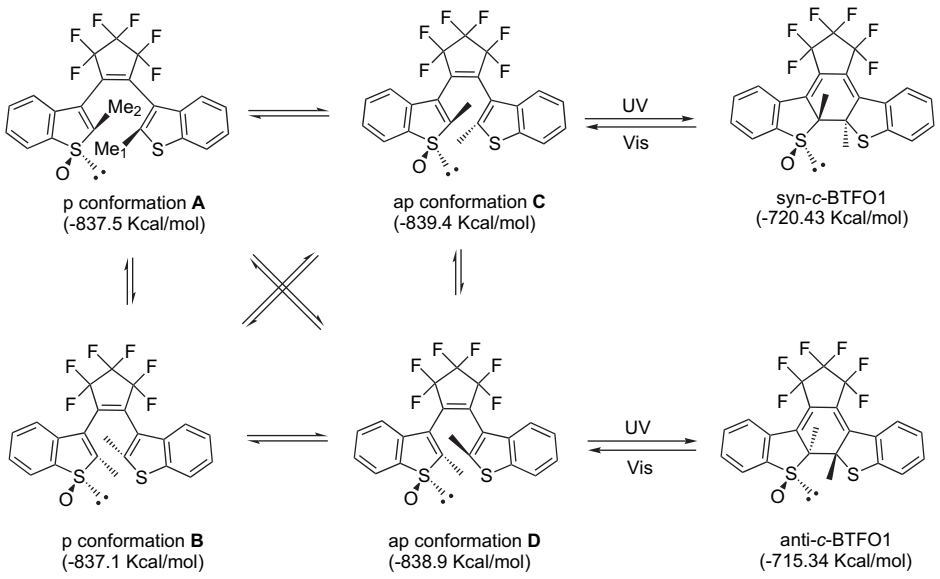

Scheme 3. Conformational isomers of o-BTFO1 and stereoisomers of c-BTFO1; those in parentheses are the heat of formation of isomers calculated using the AM1 program of MOPAC Ver 7.0.

o-BTFO1, and o-BTFO2 turned to red color solutions of their closed-ring isomers. On the other hand, colorless o-BTFO4 solution turned to yellow c-BTFO4 solution upon 312 nm lamp illumination. Upon irradiation with a visible light, those colors of closed-ring isomers were disappeared and reverted to their colorless open-ring isomers. The absorption maxima of open- and closed-ring isomers are summarized in Table 1. Interestingly, as the number of oxygen atom of the diarylethene increased, the lowest electronic absorption bands of the closed-ring isomers are blue-shifted from that of unoxidized BTF6 [523 (c-BTF6)→502 (c-BTFO1), 505 (c-BTFO2)→398 nm (c-BTFO4)]. Theoretical approach to explain the peak shift will be discussed later. The photoisomerization process was examined using HPLC analysis (silica gel column, HIQ sil C-18, eluant 2% isopropyl alcohol in hexane) to analyze the conversion ratio at the photostationary state (PSS) and the molar absorption coefficient (ε) at λ_{max} of the closed-ring isomer. HPLC chromatogram of o-BTFO1, o-BTFO2, and o-BTFO4 monitored at their isosbestic points[15] of 320, 324, and 327 nm, respectively, showed only one peak. After irradiation with a 312-nm light, BTFO2 and BTFO4 showed a new single peak. On the other hand, BTFO1 showed two new peaks because of two diastereomers of the closed-ring isomer as we discussed earlier. From the peak integration, those cyclization conversions were determined to be 0.75, 0.83, and 0.80 for BTFO1, BTFO2, and BTFO4, respectively (Table 2). It is worth noting that the conversions of BTFO*n* (*n*=1,

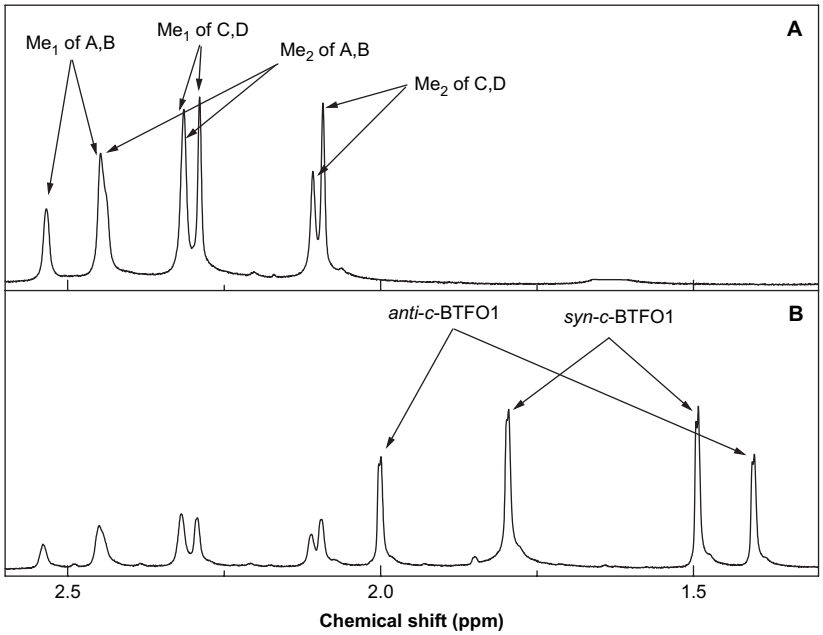

Figure 3. ^{1}H NMR (300 MHz in $CDCl_3$) of BTFO1; methyl resonances of (A) the open-ring isomer and (B) the photostationary state.

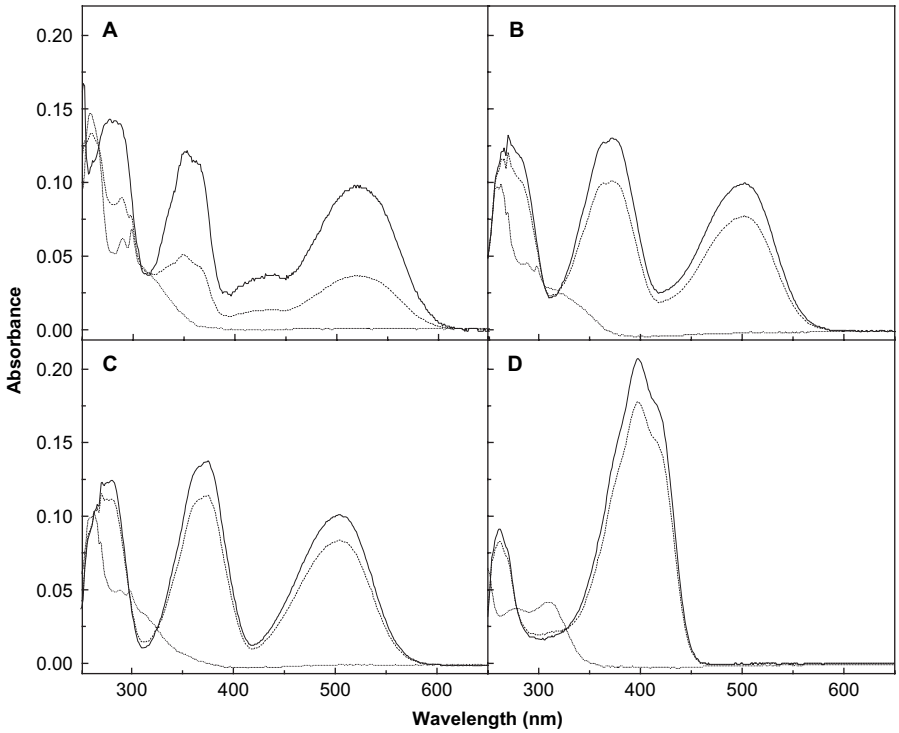

Figure 4. Absorption spectra of (A) BTF6, (B) BTFO1, (C) BTFO2, and (D) BTFO4 in ethyl acetate solution (1.0×10^{-5} M) at room temperature; open-ring isomer (dotted line) and photostationary state (dashed line) under irradiation at 312 nm, and closed-ring isomer (solid line) expected from Eq. 1.

2, and 4) at the PSS are about two times higher than that of BTF6.[6c,10] From these conversions, the absorption extinction coefficient, ε, of the closed-ring isomers at λ_{max} can be calculated using Eq. 1.[16]

$$A_{PSS} = A_{open}(1 - \text{conversion}) + A_{closed}(\text{conversion}) \qquad (1)$$

where A_{PSS}, A_{open}, and A_{closed} represent the absorbance of photostationary state, open-ring isomer, and closed-ring isomer, respectively. Table 1 shows the absorption maxima and their extinction coefficients (ε) of the open-ring isomer and the closed-ring isomer of BTF6, BTFO1, BTFO2, and BTFO4 in ethyl acetate. The quantum yields of the cyclization and ring opening of the diarylethenes at 312 nm and their absorption maxima were determined according to the literature[10c,17] and summarized in Table 2. The cyclization quantum yields of o-BTFO1 (0.39) and o-BTFO2 (0.46) were slightly higher than that of o-BTF6 (0.31). The ring-opening quantum yield of c-BTFO1, c-BTFO2, and c-BTFO4 was determined to be similar in the range of 0.061–0.074.

Table 1. Absorption maxima and extinction coefficients of BTF6, BTFO1, BTFO2, and BTFO4 in ethyl acetate, and computed absorption maxima of closed-ring forms

	λ_{max} (nm)/ε (10^{-3} M^{-1} cm^{-1})		Computed λ_{max} (nm)
	Open-ring isomer	Closed-ring isomer[a]	Closed-ring isomer
BTF6[b]	258/16.0	276/14.0	533
	290/6.2	352/12.0	
	299/6.8	523/10.0	
BTFO1	263/9.9	270/13.2	520
	290/4.5	372/13.0	
	298/4.3	502/10.0	
BTFO2	263/10.0	271/12.3	515
	289/5.0	375/13.8	
	299/4.9	505/10.0	
BTFO4	276/3.7	262/9.1	419
	308/4.1	398/21.0	

[a] Calculated from UV spectra and conversion by using Eq. 1.
[b] Taken from Ref. 6c.

2.4. Theoretical calculations

To understand the electronic transition of closed-ring isomer of BTFO*n*, theoretical calculations were performed.[18] The computed absorption wavelengths for the closed-ring isomers of BTF6, BTFO1, BTFO2, and BTFO4 are listed in Table 1. The calculations clearly demonstrate that the presence of oxygen atoms in the benzothiophene unit of the diarylethenes causes a blue shift of the first absorption maxima of the closed-ring isomer. The HOMOs and LUMOs for c-BTF6, c-BTFO1, c-BTFO2, and c-BTFO4 are plotted in Figure 5. The electron density of HOMO in c-BTF6 is

Table 2. Photochromic properties of BTF6, BTFO1, BTFO2, and BTFO4 in ethyl acetate (1.0×10^{-5} M)

	Ratio of p:ap[a]	Cyclization conversion[b,c]	Cyclization quantum yield	Ring-opening quantum yield	Fatigue time (min)
BTF6[d]	35:65	0.43	0.31	0.28	1300
BTFO1	43:57	0.75	0.39	0.072	400
BTFO2	50:50	0.83	0.46	0.074	7400
BTFO4	50:50	0.80	0.22	0.061	900

[a] Calculated from ^{1}H NMR spectra in $CDCl_3$.
[b] For all compounds, the conversion for the ring opening was 1.
[c] Calculated from HPLC.
[d] Taken from Ref. 6c.

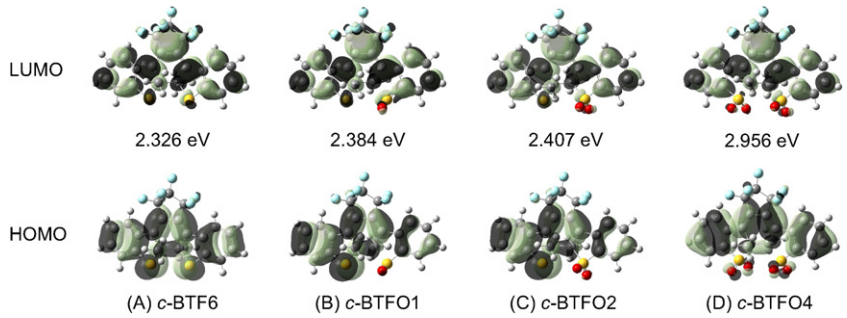

Figure 5. HOMO (bottom), LUMO (top), and energy difference between two orbitals; (A) c-BTF6, (B) c-BTFO1, (C) c-BTFO2, and (D) c-BTFO4.

well-distributed over the whole molecule including two benzothiophene rings. In the HOMO of c-BTFO1, the electron density was removed from the sulfur atom in the benzothiophene ring by oxygen. The same trend occurred in the HOMO of c-BTFO2. In c-BTFO4, since two oxygen atoms were attached to each sulfur atom of the benzothiophene rings, it is likely that only a very slight electron density remained on the sulfur atoms. However, no such change occurred in the LUMOs of these diarylethenes. Since there was only a very slight electron density on the sulfur atom in the LUMO of c-BTF6 in the beginning, it could not be removed or shifted by oxygen atoms attached to the sulfur. Interestingly, a lone-pair electron on the sulfur atom in the HOMO of c-BTF6 had an opposite sign from the neighboring electrons indicating that nodes in the electron density might be located between the sulfur and the neighboring atoms. The reduction of the electron density in the HOMO of the sulfur atom by oxidizing it to the sulfoxide or sulfone may eliminate the nodes to stabilize the HOMO. There were no such changes in the LUMOs. Thus, the stabilization of c-BTFO*n*'s HOMO can increase the energy difference between the HOMO and the LUMO, which requires more energy for electronic transition, and results in the blue-shift of the absorption bands of c-BTFO*n* as was observed experimentally.

2.5. Fluorescence properties

Figure 6 shows the steady-state fluorescence spectra of BTF6, BTFO1, BTFO2, and BTFO4 in ethyl acetate (1.0×10^{-5} M) at room temperature. Upon excitation with a 315 nm light, the emission bands of the open-ring isomer and the photostationary state (PSS) were observed. In all cases, the fluorescence intensity of each PSS was lower than that of the open-ring isomer. The open-ring isomer of BTF6 (o-BTF6) showed weak fluorescence with a band centered at 436 nm, and its PSS also showed a similar band at the same region with lower intensity (0.6 times of o-BTF6), which originates from the unreacted o-BTF6.[9d] While the fluorescence intensities of o-BTFO1 and o-BTFO2 were significantly weaker than that of o-BTF6, its intensity of o-BTFO4 was about two-fold than that of o-BTF6 when excited at 315 nm. The fluorescence spectra of BTFO4 showed that the fluorescence maxima of o-BTFO4 and its PSS were

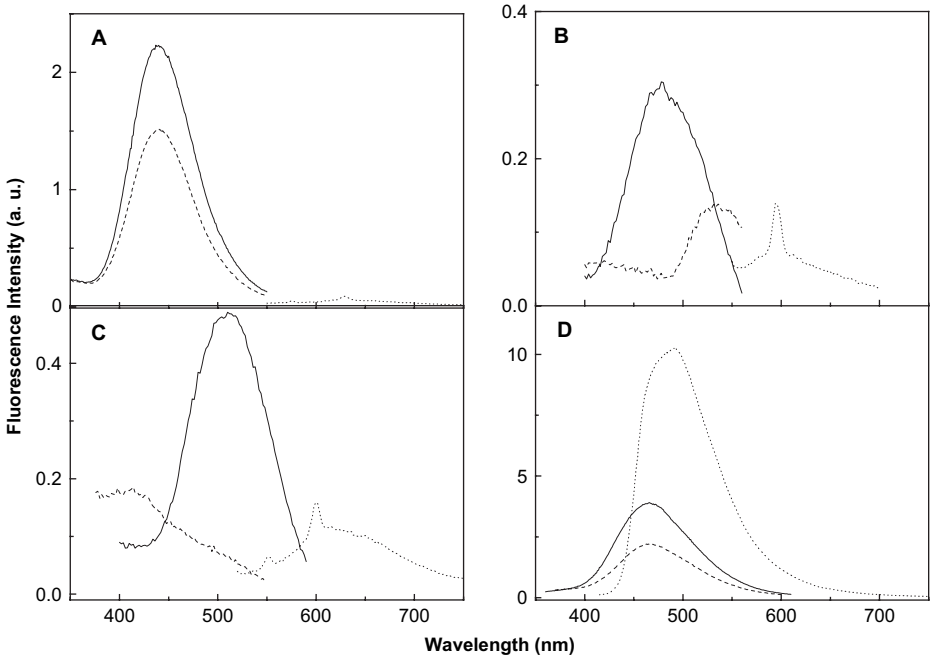

Figure 6. Emission spectra of the open-ring isomer (photoexcitation at 315 nm, solid line) and the PSS [photoexcitation at 315 nm (dashed line) and photoexcitation at the absorption maximum of each closed-ring isomer in the visible region (dotted line)] in ethyl acetate (1.0×10^{-5} M) at room temperature; (A) BTF6, (B) BTFO1, (C) BTFO2, and (D) BTFO4.

Table 3. Fluorescence properties of BTF6, BTFO1, BTFO2, and BTFO4 in ethyl acetate (1.0×10^{-5} M)

	State of diarylethene	λ_{ex} (nm)[a]	λ_{em} (nm)[b]	Φ_F[c]
BTF6	Open	315	436	0.012
BTF6	Close	540	640	—[d]
BTFO1	Open	315	486	0.0034
BTFO1	Close	502	602	—[d]
BTFO2	Open	315	510	0.0068
BTFO2	Close	505	614	—[d]
BTFO4	Open	315	464	0.025
BTFO4	Close	400	492	0.011

[a] Excitation wavelength.
[b] λ_{max} of emission band.
[c] Determined using fluoranthene (0.30:315 nm photoexcitation in cyclohexane) and 3-amino fluoranthene (0.53:400 nm photoexcitation in cyclohexane) as the reference.
[d] Not determined due to weak intensity.

observed at 464 and 470 nm in a ratio of 100:55, respectively. Since this ratio differs from the conversion ratio at the PSS, the fluorescence emission at the PSS of BTFO4 under 315 nm irradiation could be attributed to both unreacted o-BTFO4 and c-BTFO4.

The emission spectra of the closed-ring isomers with the excitation at their absorption maximum in the visible region are shown in Figure 6 as dotted lines. The fluorescence spectra of c-BTFO1 and c-BTFO2 exhibit the same general characteristics as the c-BTF6 and other diarylethenes. Surprisingly, a strong emission at 492 nm was observed for c-BTFO4 upon 400 nm light excitation.[10a] However, the fluorescence of its open-ring isomer (o-BTFO4) was not observed upon excitation with 400 nm light because of no absorption band of o-BTFO4 at this wavelength. The results of these fluorescence studies are summarized in Table 3. The fluorescence quantum yield (Φ_F) of o-BTFO4 (0.025) was higher than that of o-BTF6 (0.012) upon 315 nm light excitation. Moreover, the fluorescence intensity of c-BTFO4 (11, λ_{ex}=400 nm) was much higher than that of o-BTF6 (1.7, λ_{ex}=315 nm). There are only a few examples of diarylethenes that showed a strong emission by itself without emitter at its closed-ring state.[19] Figure 7 illustrates the photochromically driven fluorescence modulation of BTFO4 in ethyl acetate solution (1.0×10^{-5} M) recorded at 492 nm with 400 nm photoexcitation (open circle) and 470 nm with 315 nm photoexcitation (closed circle) as a function of time at room temperature. Under the excitation with 315 nm light, the fluorescence intensity of the solution was decreased to the half of o-BTFO4 during irradiation with UV light and reverted to the original intensity upon irradiation with visible light. However, under the excitation with 400 nm light, the fluorescence intensity was increased about 20 times upon UV irradiation. Even under the prolonged excitation at 400 nm for 1 h, c-BTFO4 was not converted into o-BTFO4.[10a] These results demonstrate that BTFO4 is stable under this fluorescence reading condition with a high fluorescence intensity compared with other BTF6 derivatives.

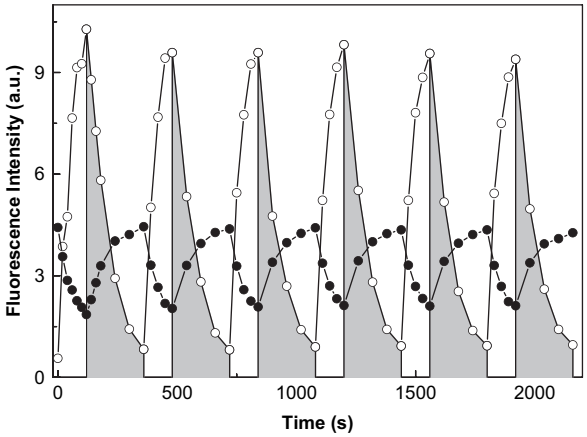

Figure 7. Modulated emission signals of BTFO4 (1.0×10^{-5} M in ethyl acetate) during alternating irradiation with 312 nm (un-shaded) and visible light (shaded). Closed circle: Ex: 315 nm, Em: 470 nm; open circle: Ex: 400 nm, Em: 492 nm.

2.6. Fatigue properties and thermal stabilities

The fatigue properties of BTF6, BTFO1, BTFO2, and BTFO4 were investigated in ethyl acetate (1.0×10^{-5} M) at room temperature using UV light irradiation. Figure 8 illustrates the absorbance changes of BTF6 (closed square), BTFO1 (closed circle), BTFO2 (open circle), and BTFO4 (open square) monitored at the λ_{max} of each closed-ring isomer as a function of the UV illumination time under air. Initially, each solution containing those diarylethenes reached the PSS (A_0) upon irradiation of UV light. Then, the absorbance of the closed-ring isomer was begun to decrease because undesirable side reactions[10b,20] were taking place to some extent under the extended irradiation with UV light. Interestingly, as shown in Figure 8, c-BTFO2 showed an excellent fatigue property compared with other BTFO*n* including BTF6 suggesting that BTFO2 is one of the most stable diarylethenes under UV light.[10b] On the other hand, partial oxidized BTFO1 has rather poor photostability compared with other BTFO*n*. These findings indicate that oxidation state of diarylethene is a key factor in determining the fatigue properties. The thermal stability of the closed-ring isomers was also investigated by storing the solutions of these diarylethenes in decaline at 80 °C under darkness. None of these materials showed any detectable change in the UV–vis spectra within a day.

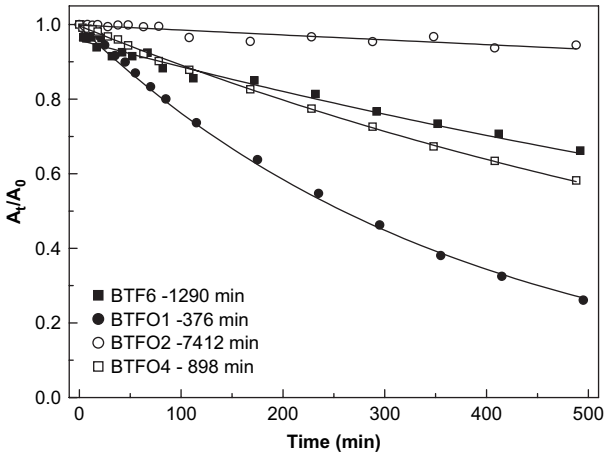

Figure 8. Absorbance changes of BTF6 (closed square), BTFO1 (closed circle), BTFO2 (open circle), and BTFO4 (open square) at the absorption maximum of each closed-ring isomer as a function of UV illumination time in ethyl acetate (1.0×10^{-5} M). The data were fitted with exponential decay (line), and the fitted data (fatigue time) represent the time in which 37% of its initial absorbance is reached under UV illumination.

3. Conclusion

The partial oxidation of BTF6 by *m*CPBA produced monosulfoxo-BTFO1 along with previously reported BTFO2 and BTFO4.[10] The compound was characterized using ^{1}H NMR, HSQC NMR, X-ray crystallography, and HRMS. We have investigated photophysical and photochromic properties of BTFO*n* including BTF6. Interestingly, the visible absorption maximum of the closed-ring isomer of BTFO*n* was shifted to the short wavelength in general as the number of oxygen was increased. Theoretical calculation suggests that this result may be explained based on the stabilization of HOMO. In the case of BTFO1, diastereoselective photocyclization was observed in 25% de, unexpectedly. More studies are needed to improve the selectivity. Oxidation state of sulfur atom in a diarylethene can play an important role in determining the photophysical and photochromic properties of photochromic materials.

4. Experimental

4.1. General methods

Octafluorocyclopentene was purchased from TCI. All other reagents were purchased from Aldrich. Melting points were taken on a Laboratory Devices Mel-Temp 3.0 melting point apparatus. The ^{1}H, ^{13}C, and HSQC NMR spectra were obtained using Jeol JNM-AL300 spectrometer at 300 and 75 MHz, and Varian AS-400 at 100 MHz, respectively, with tetramethylsilane as the internal reference. FTIR spectra were obtained using a JASCO FTIR-430. HRMS spectra were obtained on a Jeol JMS-700 spectrometer. HPLC was performed on a Young Lin SP-930D liquid chromatography coupled with a Young Lin UV-730D spectrophotometric detector. UV absorption spectra were recorded on a Shimadzu UV-3100 spectrophotometer in spectrograde ethyl acetate. Fluorescence emission spectra were recorded in spectrograde ethyl acetate on a Fluoro Max-2 spectrophotometer equipped with a 150 W ozone-free xenon lamp. UV and visible irradiations were performed with standard lamps used for visualizing TLC plates (VL6L; 312 nm, 8 mW cm^{-2}) and a 400-W tungsten lamp at room temperature. The quantum yields were measured using a 500 W Xe lamp (Newport 74000) combined with a monochromator (Newport 66921). Flash column chromatography was performed with Merck silica gel 60 (70–230 mesh). X-ray crystallographic analysis of single crystals was performed with a Bruker Smart Apex II X-ray diffractometer with Mo Kα radiation and a graphite monochromator. Crystal cell constants were calculated by global refinement. The structure was solved by direct method with SHELXS86[21a] and refined by full least squares on F^2 with SHELXL-97.[21b] CCDC-623638 (BTFO1) contained the supplementary crystallographic data for this paper. This data can be obtained free of charge from The Cambridge Crystallographic Data Center via www.ccdc.cam.ac.uk/data_request/cif.

4.2. Computational details

The Gaussian 03 program packages[22] were used for the electronic structure calculations. Geometries of BTF6, BTFO1, BTFO2, and BTFO4 were optimized at the B3LYP/6-31G(d) level. The electron density surfaces of highest occupied and lowest unoccupied molecular orbitals (HOMO and LUMO) were calculated based on these structures. The wavelengths for electronic transition were also calculated using the time-dependent density functional theory[23] (TD-DFT) at the same level.

4.3. Synthesis of 1-(2-methyl-1-benzothiophene-1-oxide-3-yl)-2-(2-methyl-1-benzothiophene-3-yl)hexafluorocyclopentene (BTFO1)

BTF6 (1.0 g, 2.1 mmol) was dissolved in CH_2Cl_2 (50 mL). The oxidant, *m*CPBA (70%, 0.70 g, 2.9 mmol) was added and stirred for 24 h at room temperature. The reaction mixture was extracted with CH_2Cl_2 (2×50 mL) and washed with aqueous Na_2SO_4 (2×50 mL). The organic layer was dried over $MgSO_4$, filtered, and the solvent was removed. The residue was purified by chromatography on silica gel to obtain BTF6 (0.26 g, 26%), BTFO1 (0.25 g, 25%), and BTFO2 (0.43 g, 41%). BTFO1, mp: 176 °C. ^{1}H NMR ($CDCl_3$, 300 MHz): δ=7.86–7.13 (m, 8H, Ar), 2.53 (s, 0.6H, p of Me_1), 2.45 (s, 1.4H, p of Me_1 and Me_2), 2.31 (s, 1.5H, p of Me_2, ap of Me_1), 2.29 (s, 0.9H, ap of Me_1), 2.11 (s, 0.7H, ap of Me_2), 2.09 (s, 0.9H, ap of Me_2). ^{1}H NMR ($CDCl_3$, 400 MHz): δ=7.83–7.12 (m, 8H, Ar), 2.52 (s, 0.6H, p of Me_1), 2.44 (s, 1.4H, p of Me_1 and Me_2), 2.32 (s, 0.8H, p of Me_2), 2.31 (s, 0.7H, ap of Me_1), 2.28 (s, 0.9H, ap of Me_1), 2.11 (s, 0.7H, ap of Me_2), 2.10 ppm (s, 0.9H, ap of Me_2). ^{1}H NMR (300 MHz, $CDCl_3$) of c-BTFO1: δ=8.27–7.13 (m, 8H), 2.00 (s, 1.1H, CH_3 of *anti*-), 1.80 (s, 1.9H, CH_3 of *syn*-), 1.49 (s, 1.9H, CH_3 of *syn*-), 1.40 ppm (s, 1.1H, CH_3 of *anti*-) (see Scheme 3 for Me_1, Me_2, *syn*- and *anti*-). FTIR (KBr cast): 3063, 3000, 2925, 2854, 1734, 1579, 1534, 1459, 1434, 1379, 1339, 1314, 1274, 1255, 1239, 1196, 1176, 1145, 1113, 1083, 1064, 1043, 995, 958, 861, 835, 825, 813, 809. HRMS (*m*/*z*) calcd for $C_{23}H_{14}F_6OS_2$: 484.0390, found: 484.0398.

Acknowledgements

This research was supported by the Korean Research Foundation (KRF-2005-005-J00801, K.-H.A., S.I.Y.), and the Ministry of Science and Technology, Korea, through the Nanotechnology Development Program (E.K.).

References and notes

1. (a) Raymo, F. M.; Tomasulo, M. *Chem. Soc. Rev.* **2005**, *34*, 327; (b) Kawata, S.; Kawata, Y. *Chem. Rev.* **2000**, *100*, 1777; (c) Kobatake, S.; Irie, M. *Annu. Rep. Prog. Chem., Sect. C* **2003**, *99*, 277; (d) Thomas, T.; Quenneville, J.; Levine, B.; Toniolo, A.; Martinez, T. J.; Lochbrunner, S.; Schmitt, M.; Shaffer, J. P.; Zgierski, M. Z.; Stolow, A. *J. Am. Chem. Soc.* **2003**, *125*, 8098; (e) Berkovic, G.; Krongauz, V.; Weiss, V. *Chem. Rev.* **2000**, *100*, 1741; (f) Delbaere, S.; Micheau, J.-C.; Frigoli, M.; Vermeersch, G. *J. Org. Chem.* **2005**, *70*, 5302; (g) Myles, A. J.; Gorodetsky, B.; Branda, N. R. *Adv. Mater.* **2004**, *16*, 922; (h) Lahav, M.; Katz, E.; Willer, I. *Langmuir* **2001**, *17*, 7387; (i) Yokoyama, Y. *Chem. Rev.* **2000**, *100*, 1717; (j) Khedhiri, L.; Corval, A.; Casalegno, R.; Rzaigui, M. *J. Phys. Chem. A* **2004**, *108*, 7434.

2. (a) Irie, M. *Chem. Rev.* **2000**, *100*, 1685; (b) Matsuda, K.; Irie, M. *J. Photochem. Photobiol., C: Photochem. Rev.* **2004**, *5*, 169; (c) Tian, H.; Yang, S. *Chem. Soc. Rev.* **2004**, *33*, 85.
3. (a) Hania, P. R.; Telesca, R.; Lucas, L. N.; Pugzlys, A.; Feringa, J.; van Esch, B. L. *J. Phys. Chem. A* **2002**, *106*, 8498; (b) Shim, S.; Joo, T.; Bae, S. C.; Kim, K. S.; Kim, E. *J. Phys. Chem. A* **2003**, *107*, 8106; (c) Murakami, M.; Miyasaka, H.; Okada, T.; Kobatake, S.; Irie, M. *J. Am. Chem. Soc.* **2004**, *126*, 14764; (d) Asano, Y.; Murakami, A.; Kobayashi, T.; Goldberg, A.; Guillaumont, D.; Yabushita, S.; Irie, M.; Nakamura, S. *J. Am. Chem. Soc.* **2004**, *126*, 12112.
4. (a) Kim, E.; Choi, Y.-K.; Lee, M.-H. *Macromolecules* **1999**, *32*, 4855; (b) Cho, S. Y.; Yoo, M.; Shin, H.-W.; Ahn, K.-H.; Kim, Y.-R.; Kim, E. *Opt. Mater.* **2002**, *21*, 279; (c) Bertarelli, C.; Bianco, A.; Amore, F. D.; Gallazzi, M. C.; Zerbi, G. *Adv. Funct. Mater.* **2004**, *14*, 357; (d) Kim, M.-S.; Maruyama, H.; Kawai, T.; Irie, M. *Chem. Mater.* **2003**, *15*, 4539.
5. (a) Wigglesworth, T. J.; Sud, D.; Norsten, T. B.; Lekhi, V. S.; Branda, N. R. *J. Am. Chem. Soc.* **2005**, *127*, 7272; (b) de Jong, J. J. D.; Lucas, L. N.; Kellogg, R. M.; van Esch, J. H.; Feringa, B. L. *Science* **2004**, *304*, 278; (c) Kose, M.; Shinoura, M.; Yokoyama, Y.; Yokoyama, Y. *J. Org. Chem.* **2004**, *69*, 8403; (d) Yamaguchi, T.; Nomiyama, K.; Isayama, M.; Irie, M. *Adv. Mater.* **2004**, *16*, 643; (e) Yokoyama, Y.; Shiraishi, H.; Tani, Y.; Yokoyama, Y.; Yamaguchi, Y. *J. Am. Chem. Soc.* **2003**, *125*, 7194; (f) Murguly, E.; Norsten, T. B.; Branda, N. R. *Angew. Chem., Int. Ed.* **2001**, *40*, 1752; (g) Kodani, T.; Matsuda, K.; Yamada, T.; Kobatake, S.; Irie, M. *J. Am. Chem. Soc.* **2000**, *122*, 9631; (h) Yamaguchi, T.; Uchida, K.; Irie, M. *J. Am. Chem. Soc.* **1997**, *119*, 6066; (i) Yamaguchi, T.; Inagawa, T.; Nakazumi, H.; Irie, S.; Irie, M. *Chem. Mater.* **2000**, *12*, 869; (j) Yamaguchi, T.; Inagawa, T.; Nakazumi, H.; Irie, S.; Irie, M. *J. Mater. Chem.* **2001**, *11*, 2453; (k) Uchida, K.; Walko, M.; de Jong, J. J. D.; Sukata, S.; Kobatake, S.; Meetsma, A.; van Esch, J.; Feringa, B. L. *Org. Biomol. Chem.* **2006**, *4*, 1002.
6. (a) Matsuda, K.; Irie, M. *J. Am. Chem. Soc.* **2000**, *122*, 7195; (b) Takayama, K.; Matsuda, K.; Irie, M. *Chem.—Eur. J.* **2003**, *9*, 5605; (c) Matsuda, K.; Irie, M. *Tetrahedron Lett.* **2000**, *41*, 2577.
7. (a) de Jong, J. J. D.; Browne, W. R.; Walko, M.; Lucas, L. N.; Barrett, L. J.; McGarvey, J. J.; van Esch, J. H.; Feringa, B. L. *Org. Biomol. Chem.* **2006**, *4*, 2387; (b) Bianco, A.; Bertarelli, C.; Rabolt, J. F.; Zerbi, G. *Chem. Mater.* **2005**, *17*, 869; (c) Chen, Y.; Xie, N. *J. Mater. Chem.* **2005**, *15*, 3229; (d) Uchida, K.; Saito, M.; Murakami, A.; Kobayashi, T.; Nakamura, S.; Irie, M. *Chem.—Eur. J.* **2005**, *11*, 534; (e) Uchida, K.; Takata, A.; Saito, M.; Murakami, A.; Nakamura, S.; Irie, M. *Adv. Funct. Mater.* **2003**, *13*, 755; (f) Stellacci, F.; Bertarelli, C.; Toscano, F.; Gallazzi, M. C.; Zerbi, G. *Chem. Phys. Lett.* **1999**, *302*, 563.
8. (a) Gorodetsky, B.; Samachetty, H. D.; Donkers, R. L.; Workentin, M. S.; Branda, N. R. *Angew. Chem., Int. Ed.* **2004**, *43*, 2812; (b) Gilat, S. L.; Kawai, S. H.; Lehn, J.-M. *Chem.—Eur. J.* **1995**, *1*, 275.
9. (a) Golovkova, T. A.; Kozlov, D. V.; Neckers, D. C. *J. Org. Chem.* **2005**, *70*, 5545; (b) Fukaminato, T.; Sasaki, T.; Kawai, T.; Tamai, N.; Irie, M. *J. Am. Chem. Soc.* **2004**, *126*, 14843; (c) Irie, M.; Fukaminato, T.; Sasaki, T.; Tamai, N.; Kawai, T. *Nature* **2002**, *420*, 759; (d) Cho, H.; Kim, E. *Macromolecules* **2002**, *35*, 8684; (e) Norsten, T. B.; Branda, N. R. *Adv. Mater.* **2001**, *13*, 347; (f) Norsten, T. B.; Branda, N. R. *J. Am. Chem. Soc.* **2001**, *123*, 1784; (g) Kawai, T.; Kim, M.-S.; Sasaki, T.; Irie, M. *Opt. Mater.* **2002**, *21*, 275; (h) Kawai, T.; Sasaki, T.; Irie, M. *Chem. Commun.* **2001**, 711; (i) Giordano, L.; Jovin, T. M.; Irie, M.; Jares-Erijman, E. A. *J. Am. Chem. Soc.* **2002**, *124*, 7481; (j) Lim, S.-J.; An, B.-K.; Jung, S. D.; Chung, M.-A.; Park, S. Y. *Angew. Chem., Int. Ed.* **2004**, *43*, 6346; (k) Osuka, A.; Fujikane, D.; Shinmori, H.; Kobatake, S.; Irie, M. *J. Org. Chem.* **2001**, *66*, 3913; (l) Jiang, G.; Wang, S.; Yuan, W.; Jiang, L.; Song, Y.; Tian, H.; Zhu, D. *Chem. Mater.* **2006**, *18*, 235.
10. (a) Jeong, Y.-C.; Yang, S. I.; Ahn, K.-H.; Kim, E. *Chem. Commun.* **2005**, 2503; (b) Jeong, Y.-C.; Park, D. G.; Kim, E.; Ahn, K.-H.; Yang, S. I. *Chem. Commun.* **2006**, 1881; (c) Jeong, Y.-C.; Yang, S. I.; Kim, E.; Ahn, K.-H. *Tetrahedron* **2006**, *62*, 5855.
11. Hanazawa, M.; Sumiya, R.; Horikawa, Y.; Irie, M. *J. Chem. Soc., Chem. Commun.* **1992**, 206.
12. (a) Takeshita, M.; Choi, C. N.; Irie, M. *Chem. Commun.* **1997**, 2265; (b) Takeshita, M.; Kato, N.; Kawauchi, S.; Imase, T.; Watanabe, J.; Irie, M. *J. Org. Chem.* **1998**, *63*, 9306; (c) Takeshita, M.; Nagai, M.; Yamato, T. *Chem. Commun.* **2003**, 1496.
13. Corma, A.; Garcia, H. *Chem. Rev.* **2002**, *102*, 3837.
14. Uchida, K.; Tsuchida, E.; Aoi, Y.; Nakamura, S.; Irie, M. *Chem. Lett.* **1999**, 63.
15. Kaieda, T.; Kobatake, S.; Miyasaka, H.; Murakami, M.; Iwai, N.; Nagata, Y.; Itaya, A.; Irie, M. *J. Am. Chem. Soc.* **2002**, *124*, 2015.
16. Frigoli, M.; Mehi, G. H. *Chem.—Eur. J.* **2004**, *10*, 5243.
17. (a) Nakashima, H.; Irie, M. *Macromol. Chem. Phys.* **1999**, *200*, 683; (b) Nakashima, H.; Irie, M. *Polym. J.* **1998**, *30*, 985.
18. (a) Clark, A. E. *J. Phys. Chem.* **2006**, *110*, 3790; (b) Jacquemin, D.; Perpete, E. A. *Chem. Phys. Lett.* **2006**, *429*, 147.
19. (a) Fernandez-Acebes, A.; Lehn, J.-M. *Chem.—Eur. J.* **1999**, *5*, 3285; (b) Kim, M.-S.; Kawai, T.; Irie, M. *Opt. Mater.* **2002**, *21*, 271.
20. (a) Peters, A.; Branda, N. R. *Adv. Mater. Opt. Electron.* **2000**, *10*, 245; (b) Higashiguchi, K.; Matsuda, K.; Kobatake, S.; Yamada, T.; Kawai, T.; Irie, M. *Bull. Chem. Soc. Jpn.* **2000**, *73*, 2389; (c) Irie, M.; Lifka, T.; Uchida, K.; Kobatake, S.; Shindo, Y. *Chem. Commun.* **1999**, 747; (d) Jeong, Y.-C.; Kim, E.; Ahn, K.-H.; Yang, S. I. *Bull. Korean Chem. Soc.* **2005**, *26*, 1675.
21. (a) Sheldrick, G. M. *Acta Crystallogr., Sect. A* **1990**, *46*, 467; (b) Sheldrick, G. M. *SHELXL-97, Program for Crystal Structure Refinement*; Universität Göttingen: Göttingen, Germany, 1997.
22. Frisch, M. J.; Trucks, G. W.; Schlegel, H. B.; Scuseria, G. E.; Robb, M. A.; Cheeseman, J. R.; Montgomery, J. A.; Vreven, T., Jr.; Kudin, K. N.; Burant, J. C.; Millam, J. M.; Iyengar, S. S.; Tomasi, J.; Barone, V.; Mennucci, B.; Cossi, M.; Scalmani, G.; Rega, N.; Petersson, G. A.; Nakatsuji, H.; Hada, M.; Ehara, M.; Toyota, K.; Fukuda, R.; Hasegawa, J.; Ishida, M.; Nakajima, T.; Honda, Y.; Kitao, O.; Nakai, H.; Klene, M.; Li, X.; Knox, J. E.; Hratchian, H. P.; Cross, J. B.; Bakken, V.; Adamo, C.; Jaramillo, J.; Gomperts, R.; Stratmann, R. E.; Yazyev, O.; Austin, A. J.; Cammi, R.; Pomelli, C.; Ochterski, J. W.; Ayala, P. Y.; Morokuma, K.; Voth, G. A.; Salvador, P.; Dannenberg, J. J.; Zakrzewski, V. G.; Dapprich, S.; Daniels, A. D.; Strain, N. C.; Farkas, O.; Malick, D. K.; Rabuck, A. D.; Raghavachari, K.; Foresman, J. B.; Ortiz, J. V.; Cui, Q.; Baboul, A. G.; Clifford, S.; Cioslowski, J.; Stefanov, B. B.; Liu, G.; Liashenko, A.;

Piskorz, P.; Komaromi, I.; Martin, R. L.; Fox, D. J.; Keith, T.; Al-Laham, M. A.; Peng, C. Y.; Nanayakkara, A.; Challacombe, M.; Gill, P. M. W.; Johnson, B.; Chen, W.; Wong, M. W.; Gonzalez, C.; Pople, J. A. *Gaussian 03, Revision C.02*; Gaussian: Wallingford, CT, 2004.

23. (a) Stratmann, R. E.; Scuseria, G. E.; Frisch, M. J. *J. Chem. Phys.* **1998**, *109*, 8218; (b) Bauernschmitt, R.; Ahlrichs, R. *Chem. Phys. Lett.* **1996**, *256*, 454; (c) Casida, M. E.; Jamorski, C.; Casida, K. C.; Salahub, D. R. *J. Chem. Phys.* **1998**, *108*, 4439.